Technische Universiteit
Eindhoven
University of Technology

Department of Electrical Engineering

Den Dolech 2, 5612 AZ Eindhoven
P.O. Box 513, 5600 MB Eindhoven
The Netherlands
http://w3.ele.tue.nl/nl/

Series title:
Master graduation paper,
Electrical Engineering

Commissioned by Professor:
prof. dr. A.G. Tijhuis

Group / Chair:
Electromagnetics

Date of final presentation:
June 18, 2015

Report number:

The Effect of Transcranial Magnetic Stimulation on the Functional Connectivity of the Brain

by

Author: S. de Haan

Internal supervisors: D.C.W. Klooster MSc. PDEng,
prof. dr. A.P. Aldenkamp, prof. dr. A.G. Tijhuis

The Effect of Transcranial Magnetic Stimulation on the Functional Connectivity of the Brain

S. de Haan

***Abstract*—A pipeline for the analysis of the effect of transcranial magnetic stimulation (TMS) on the functional connectivity (FC) was created. The results of the pipeline for a single subject are presented. A subject with major depressive disorder underwent four consecutive days of intermittent theta burst stimulation (iTBS) at the left dorsolateral prefrontal cortex (DLPFC), at 100% motor threshold. Magnetic resonance imaging (MRI) was performed before and after the stimulation protocol. Derived from resting state functional MRI the FC was determined for the whole brain, the default mode network (DMN) and the central executive network (CEN). The characteristic path length and clustering coefficient were extracted from the derived binary and weighted graphs. Seed-to-voxel analysis was performed to determine the FC between the seed, the DLPFC, and the voxels of the DMN and CEN. After TMS the average connectivity was decreased and the connectivity change per node indicated a spread of the effect over the whole brain. The weighted graph parameters for the whole brain and the DMN showed increased path lengths and decreased clustering coefficients. The other parameters did not indicate an effect. Seed-to-voxel analysis indicated a decreased connectivity between the DLPFC and the CEN. The analysis of more subjects and further research is needed before conclusions can be drawn.**

***Index Terms*—fMRI, functional connectivity, transcranial magnetic stimulation.**

I. Introduction

TRANSCRANIAL magnetic stimulation (TMS) is a non-invasive and almost pain free neuromodulation technique that is used to modulate neural networks of the brain. During TMS, an alternating current is sent through a coil placed at the scalp which induces a current in the brain by electromagnetic induction. TMS is increasingly used for stimulation of the human brain to study brainbehavior relations, the pathophysiology of diseases and the potential of neuromodulation for rehabilitation and therapy [22]. Research on the therapeutic benefits, in multiple neurological conditions, is ongoing. It has shown positive effects in persons with e.g. depression and is being investigated for use with epilepsy [10], [11].

High frequency TMS of 10 Hz applied at the left dorsolateral prefrontal cortex (DLPFC) has shown positive effects on patients with depression [11], [23]. Low frequency TMS applied at the right DLPFC showed similar positive effects [15]. However the mechanism of action of TMS remains unclear. The effect of treatment is hard to predict and comparison between studies is difficult due to the variety in stimulation parameters such as frequency, stimulation protocol and stimulation site. It is important to gain more insight in the mechanisms of TMS to be able to optimize stimulation parameters and increase therapeutic efficacy.

The general goal is a complete understanding of the effect of electromagnetic fields on the brain. To gain a better understanding on how TMS affects the brain, the current research aims at determining the effect of TMS on functional connectivity (FC).

Studies by Liston et al. [12] and Salomons et al. [17] investigated the effect of TMS on the FC derived from functional magnetic resonance imaging (MRI) in patients with major depressive disorder (MDD). Liston et al. showed the elevated connectivity within the default mode network (DMN) was normalized after TMS. The diminished connectivity in the central executive network (CEN) did not change. Salomons et al. found that localized connectivity was associated with successful treatment response. Shafi et al. investigated the effect on FC derived from electroencephalography (EEG) using graph theory [18]. Their research showed the FC after stimulation was modulated which was also indicated by the adjusted graph parameters.

The goal of this project was to develop an analysis pipeline to process resting state fMRI data and calculate graph parameters for FC derived from this data. The analysis pipeline was tested using a dataset of a single subject with MDD that underwent intermittent theta burst stimulation (iTBS) applied at the DLPFC. The iTBS protocol has shown to facilitate the motor evoked potential when applied at the motor cortex [7]. When applied at the DLPFC this might be used to compensate the diminished activity in the DLPFC in patients with MDD [13]. The hypothesis was that FC is affected after TMS. The direct effect was expected close to the stimulation area, together with an indirect effect which spreads along the networks comprising this area. To test the hypothesis FC analysis were performed and using graph theory network parameters were extracted. This was done for the entire brain and two specific networks: the DMN and CEN, which have shown abnormal FC in depression [12].

In Section II the theory of FC and graph theory is described. In Section III the analysis pipeline is presented, consisting of the preprocessing steps and the calculated parameters. The results are presented in Section IV. Section V contains the discussion, Section VI contains the conclusion and recommendations.

II. Theory

A. Functional Connectivity

In this research the FC was investigated. FC is the connectivity between brain areas that share functional properties. This implies that functionally connected brain areas are simultaneously activated and therefore related time series can be measured in those regions. The FC is measured with resting state fMRI using the blood-oxygen-level dependent (BOLD)

contrast. In resting state fMRI no specific task is performed, the subject lies still in the scanner and spontaneous brain activity is measured. The BOLD contrast is based on the different magnetization between oxygen-rich and oxygen-poor blood. Activated neurons require an increase in oxygen flow which results in a change in local magnetization. This local magnetization change can be measured by fMRI and is a measure for the ratio of oxygen-rich and oxygen-poor blood and therefore a measure of local brain activity. The fMRI scans are used to analyze which areas of the brain are active at the same time and therefore assumed to be connected.

The connection strength is determined by calculating the pairwise correlations between all regions using Pearson's correlation coefficient (1), followed by Fisher's z-transform (2) to normalize the distribution.

$$r = \mathrm{corr}(\mathrm{X}, \mathrm{Y}) = \frac{\sum_{\mathrm{i}=1}^{\mathrm{n}} (\mathrm{X_i} - \bar{\mathrm{X}})(\mathrm{Y_i} - \bar{\mathrm{Y}})}{\sqrt{\sum_{\mathrm{i}=1}^{\mathrm{n}} (\mathrm{X_i} - \bar{\mathrm{X}})^2} \sqrt{\sum_{\mathrm{i}=1}^{\mathrm{n}} (\mathrm{Y_i} - \bar{\mathrm{Y}})^2}} \quad (1)$$

$$z = \frac{1}{2} \ln \left(\frac{1 + \mathrm{r}}{1 - \mathrm{r}} \right) = \mathrm{arctanh(r)} \quad (2)$$

Here X and Y are time series of length n, $\bar{X}$ and $\bar{Y}$ are the mean values of X and Y.

The analysis of FC can indicate disorders and might improve diagnosis, e.g. of epilepsy [5] and depression [28]. It is shown the FC differs in people with MDD and the abnormalities are found both in the DMN and the CEN [12]. The FC of the subgenual cingulate and thalamus with the DMN has shown to be significantly increased [6]. The FC in the DMN has shown to be increased and the FC in the CEN is decreased. TMS has shown to modulate the FC in the DMN and between the DMN and CEN in depressed people [12].

B. Graph Theory

Graph theory is the study of graphs, the mathematical structures consisting of nodes and edges. Graph theory is used to characterize FC networks based on their topology [21], [25]. Graph theory of resting state fMRI can be used to assist diagnosis for Alzheimer's disease [9].

In this research the graphs are used to represent the FC in the brain. The anatomical regions are represented by nodes in the graph and the edges show the functional connections between the nodes. A graph is described by the nodes, its edges and possibly the weight of the edges. When no weighting is applied and the edges have uniform strength, it is called a binary graph. When weighting is applied to the edges it is a weighted graph. Both types of graphs are used in this research. The used graphs are undirected as there is no direction in the connectivity.

The graphs are derived from the functional connection strengths. The binary graphs are constructed by applying a threshold which removes all connections below the threshold. The strongest connections above the threshold result in edges with uniform weight in the graph. This enhances the contrast between strong and week connections. This in contrast to the weighted graphs, where the connection strengths are used as weights for the edges and only the negative connections are removed.

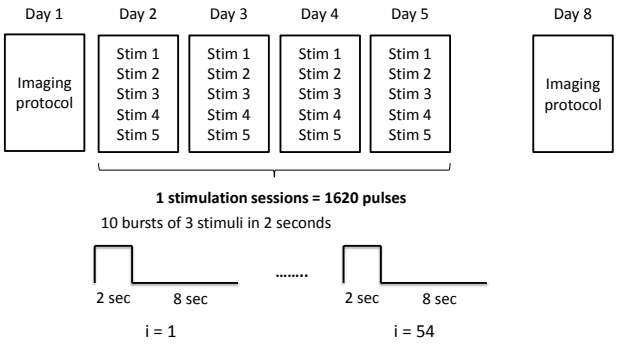

Fig. 1. Overview of the stimulation protocol. The first day the subject is scanned, followed by four days of stimulation of 5 sessions a day. On the eight day the subject is rescanned.

The properties of these graphs are expressed by certain parameters [16]. The calculated parameters are the characteristic path length (L) and the clustering coefficient (C). The characteristic path length is the average shortest path length, the clustering coefficient is a measure for the overall clustering in the graph. The path length L is calculated for both binary and weighted graphs. The binary clustering coefficient C^b differs from the the weighted clustering coefficient C^w. The parameters are calculated as follows:

$$L = \frac{1}{n(n-1)} \sum_{i,j \in G, i \neq j} d_{i,j} \quad (3)$$

$$C^b = \frac{1}{n} \sum_{i \in G} \frac{\sum_{j,h \in G} (a_{i,j} a_{j,h} a_{h,i})}{k_i (k_i - 1)} \quad (4)$$

$$C^w = \frac{1}{n} \sum_{i \in G} \frac{\sum_{j,m \in G} (w_{i,j} w_{j,h} w_{h,i})^{1/3}}{k_i (k_i - 1)} \quad (5)$$

Here $d_{i,j}$ is the shortest distance between node i and j, n is the total number of nodes in the graph. $a_{i,j}$ is the binary connection strength so either 0 or 1, $w_{i,j}$ the weighted connection strength and k_i is the sum of connection strengths originating from node i.

The graph parameters depend highly on the number of edges in the graph [21]. Hence to be able to compare the parameters derived from the binary graphs, the number of edges in the compared graphs is chosen to be equal. For the weighted graphs the number of edges is directly dependent of the connection strengths and therefore the total connection strength can differ between the two graphs.

For the parameters to be meaningful, it is important that all nodes are connected such that every node can reach every other node via a certain, not necessarily direct, path. Unconnected nodes would result in an infinite characteristic path length, independent of the rest of the network.

III. Analysis Pipeline

A single subject with MDD underwent four consecutive days of iTBS applied at the left dorsolateral prefrontal cortex

(DLPFC). A day before the first stimulation session the subject was scanned using a Siemens MRI of 3T, where the used parameters were a 2000ms repetition time, an echo time of 29 ms and a flip angle of 90 degrees. The next four days after the scanning protocol the stimulation was applied. The iTBS was applied with a Magstim Rapid2 Plus1 magnetic stimulator (Magstim Company Limited, Wales, UK) with a figure-of-eight coil. The resting motor threshold (MT) was determined on the right abductor pollicis brevis muscle. Each day of stimulation consisted of 5 sessions where each session contained 54 bursts of 10 pulse trains of 3 at 100% MT. This resulted in 1620 pulses per session. Exactly one week after the first scan the subject was rescanned. An overview of the protocol is shown in Figure 1.

The data were processed using MATLAB R2014b (The MathWorks Inc., Natick, MA, US) with the conn toolbox [26] and SPM12 (Wellcome Trust Centre for Neuroimaging, London, UK).

A. Preprocessing fMRI data

The fMRI data were preprocessed to increase the signal to noise ratio by correcting for movement, scanner artifacts and other uncontrollable variance. A schematic overview of the applied preprocessing steps in SPM is shown in Figure 2.

At the beginning of a scan start-up effects can appear. The tissue is adjusting to the large signal change which results in higher contrast in the first scans due to magnetic saturation effects. Dummy scans are used to allow magnetization equilibrium to be reached before data is acquired. As it was unsure if dummy lead-in scans were used, start-up effects might affect the measurements in the first scans and therefore the first 10 measurements were discarded. The remaining fMRI images were realigned, slice time corrected, coregistered, segmented, spatially normalized and smoothed using SPM:

1) Slice Timing Correction: Slice timing correction corrects for the time differences as a function of acquisition order between different slices of the same scan. The slices were acquired in an interleaved order which creates a timing difference of half the repetition time between two adjacent slices. Using interpolation the signals were corrected for not acquiring every slice in a volume at the same time.

2) Realignment: In this step the functional images were individually realigned to correct for movement of the subject which would result in errors in the time series. Rigid body transformations, translations and rotations in three directions, were used to minimize movement effects. A mean image was created for coregistering.

3) Coregistering: Coregistering matches the structural MRI scan to the functional MRI scans by maximizing the mutual information between the structural image and the mean functional image. As the functional scans were already realigned, the structural and functional scans are all in the same space after coregistering. Only rigid body transformations were used in this step.

4) Segmentation: Segmentation uses the structural scan to derive images for each of the three different tissue types: gray matter (GM), white matter (WM) and cerebrospinal fluid (CSF). Segmentation also creates a deformation field that is used for normalization. The structural image was matched to tissue probability maps. These maps are in a standard coordinate system, the MNI space, which is a standardized brain template from the Montreal Neurological Institute and Hospital. The tissue probability maps were used together with the information in the structural image to create the segmented images. To match the structural image to the tissue probability maps, the structural image was transformed to the same space as the probability maps. The used transformation was stored in the deformation field.

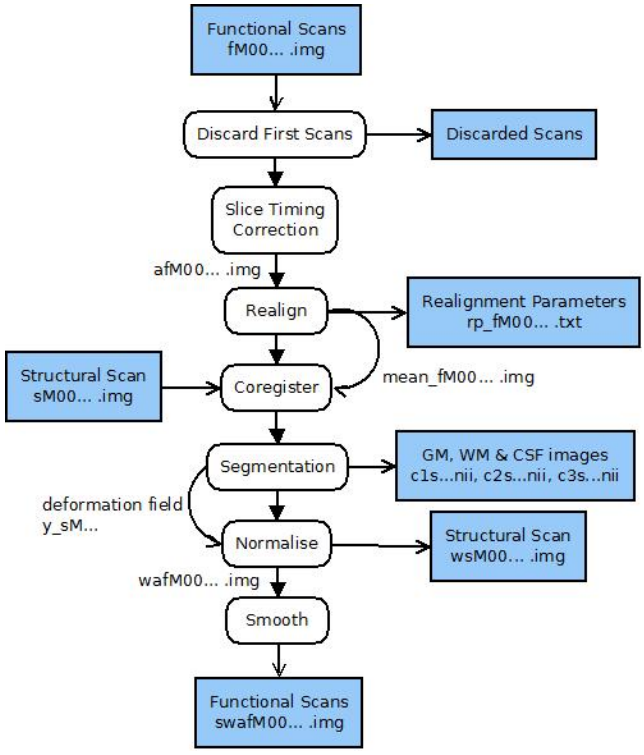

Fig. 2. The preprocessing pipeline created for SPM. The white blocks represent the processing steps, the blue blocks are the in- and outputs.

5) Normalization: Normalization transformed the scans into the standardized MNI space. This was done by applying the transformations stored in the deformation field to all the required scans. Normalization is required to be able to compare scans of different subjects. Translations, rotations, zooms and nonlinear deformations were used.

6) Smoothing: The scans were spatially smoothed using a Gaussian kernel with a full width half maximum of 6 mm, twice the voxel size, to correct for slight remaining functional/anatomical differences and decrease spatial noise.

After preprocessing in SPM, the signals were denoised using the Matlab toolbox conn. The realignment parameters and signals derived from the WM and CSF voxels were used as regressors in the general linear model to clean up the data. Even though realignment was applied, it can not be assumed that all movement effects were removed from the signal. In the WM and CSF there are no cell bodies and the signals measured there are not directly caused by brain activity. Therefore they were considered noise and were used to model the noise in

the entire scan. The noise was modeled with the aCompCor algorithm [3]. For both CSF and WM the 5 strongest time serie components, derived using principal component analysis, were used as regressors. The global signal was not used as regressor. Finally, a bandpass filter ranging from 0.1 to 0.01 Hz was applied to filter out cardiac and respiratory cycle disturbances and low frequency scanner drift.

B. Calculated Parameters

1) Functional connectivity matrices: The brain was split into 84 regions by the Brodmann atlas [4]. The atlas is based on the cellular composition of the brain and the individual areas can be linked to certain brain functions. The stimulation region consisted of the two Brodmann Areas (BA) 9 and 46 in the left hemisphere that together form the left DLPFC. These two regions were combined and further referred to as the seed region. The time-series were calculated for all the 83 individual regions (as listed in Appendix A). This was done by averaging over all individual voxel signals in the region. Here the unsmoothed voxel time-series were used to prevent potential loss of the BOLD signal by contamination of nearby areas.

The FC was calculated between all 83 regions and the calculated correlation values were ordered in the 83 by 83 FC matrices for pre and post TMS. The difference between the matrices was visualized and calculated as difference = post FC - pre FC. To determine an overall connectivity change a one-tailed paired t-test with $p < 0.05$ was done over all undoubled elements of the matrix to compare the average FC before and after stimulation.

To determine local effects in the connectivity change, the connectivity change per node was calculated by comparing the rows of the connectivity matrices individually. Every row consists of the connection strengths from a single area with all other areas. A one-tailed paired t-test (with $p < 0.05$, corrected for multiple comparisons using Bonferroni correction) was performed over the two corresponding rows from before and after TMS. A schematic overview of this measure is shown in Figure 3.

2) Graph parameters: Graph theory was first applied to analyze the whole brain. The graphs were derived from the 83 by 83 FC matrices.

The parameters were calculated for the binary and weighted graphs. The binary graphs were constructed using a sparsity of 0.3 such that 70 percent of all possible connections were present. This value was determined by calculating the minimum number of connections necessary to achieve connected graphs. This gave a value just below 70 percent, which was rounded upwards and set for the two graphs, pre and post, such that both graphs have an equal amount of edges. The 30 percent weakest connections were removed by setting the connection strengths to 0. Then using formulas 3 and 4 the binary L and C^b were calculated.

The weighted graphs were determined by using all the positive connection strengths. The interpretation of negative correlation strengths is not straightforward and therefore the negative connections were set to 0 [16]. The positive connection strengths were kept unchanged. From the resulted connectivity matrix the weighted C^w is calculated. The distance between two connected nodes was determined as the inverse of the connectivity coefficient. The calculated distance matrix was used to calculate L. The parameter calculations were derived from the Brain Connectivity Toolbox [16].

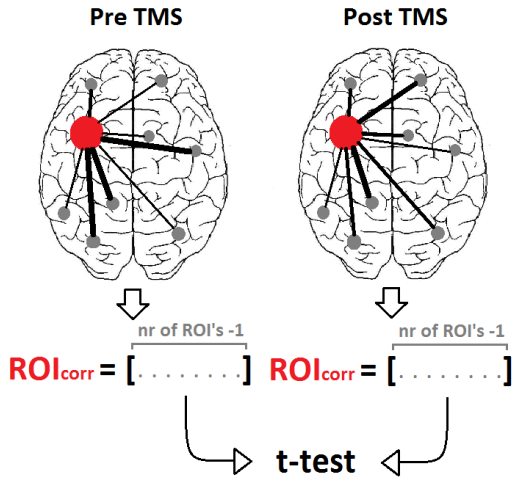

Fig. 3. Schematic overview of the calculation of the local connectivity change. For a node, shown in red, the correlation values with all other nodes are stored in an array, ROIcorr. This is done separately for pre and post. Then a t-test is done over the arrays.

After the whole brain analysis, the graph analysis was repeated for selected brain networks on a voxel-to-voxel level. Analyzing over the full brain might average out the effects of TMS. Therefore the individual networks were analyzed to investigate the spatial distribution of the effect. The analysis was performed on the regions of the DMN and the CEN.

To determine the areas involved in these networks, resting state network masks from a study by Smith et al. [19] were used. In this study independent component analysis was performed on temporally concatenated resting state data of 36 subjects. These resting state networks were matched with the networks from the BrainMap database consisting of 29,671 subjects. A threshold of Z = 3 was applied to create binary masks. The resulting Smith masks are shown in Figure 4.

The correlation matrices on a voxel-to-voxel level were calculated and the binary graphs were constructed with a sparsity of 0.8, the maximum value which resulted in a connected graph, resulting in 20 percent of all possible connections. The binary parameters were extracted. Also the weighted parameters were determined from the correlation matrices where all negative connections were set to 0.

3) Seed-to-voxel analysis: To determine the connectivity between the TMS seed and the networks, the seed-to-voxel analysis from the DLPFC to the DMN and the CEN was calculated. The average time serie of the DLPFC was correlated with all voxels in the DMN and the CEN. The binary Smith masks for the CEN and DMN were used. The connectivity change was determined by calculating the difference between pre and post analysis. As the DLPFC is part of the CEN, the seed-to-voxel analysis between the DLPFC and the CEN gave

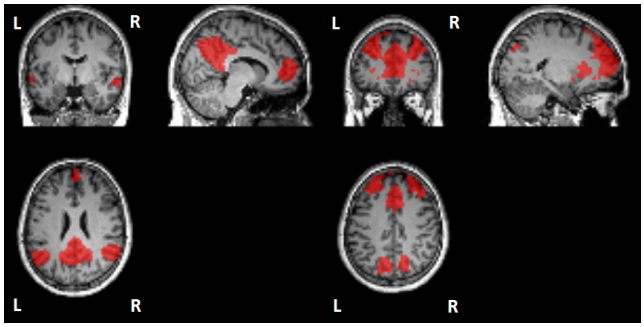

Fig. 4. Masks for the Default Mode Network and the Central Executive Network. The masks were derived from a study of Smith et al [ref],which resulted in 10 resting state networks well-matched to components of the 29,671-subject BrainMap activation database. The masks were thresholded at Z = 3.

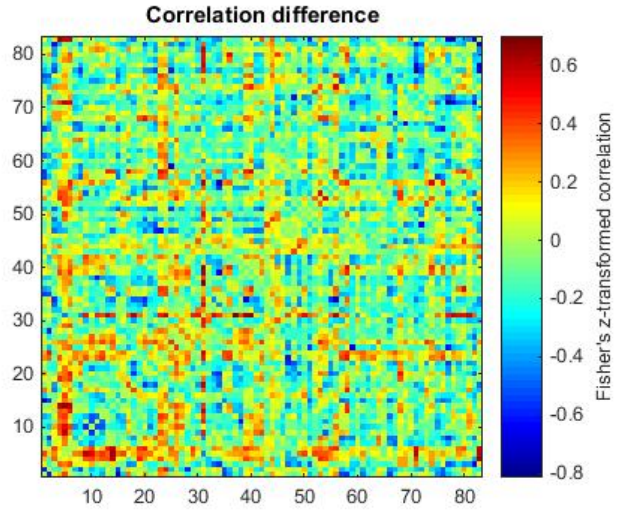

Fig. 5. The difference of the functional connectivity matrices, calculated as post TMS minus pre TMS, in Fisher z-transformed correlation coefficient. The indices along the axes correspond to the 83 brain areas listed in Appendix A. Some areas show an increased connectivity, most areas show a connectivity decrease.

a measure for the within-network connectivity of the CEN. The analysis between the DLPFC and the DMN gave a measure of connectivity between the TMS seed and the DMN.

IV. Results

A. Functional connectivity matrices

The FC matrices showed the overall FC was significantly decreased after stimulation ($p = 3 \cdot 10^{-34}$). The difference matrix is shown in Figure 5.

The connectivity change per node is shown in Figure 6. In line with the overall FC change most nodes showed a decreased connectivity. 33 nodes showed a significant decreased connectivity after stimulation, 9 nodes an increased connectivity. The other 41 nodes showed no significant change. The TMS seed showed a decreased connectivity. The affected nodes were almost equally distributed over left and right hemispheres (4 left versus 5 right increased, 22 versus 19 decreased).

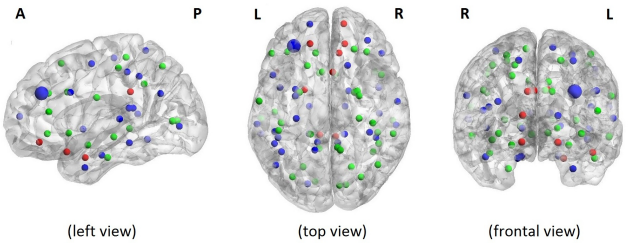

Fig. 6. Connectivity change per node. The left view, top view and frontal view are shown. The larger node represents the TMS seed, the dorsolateral prefrontal cortex. The 33 blue nodes represent a significant decreased connectivity, the 9 red nodes an increased connectivity. 41 green nodes showed no significant connectivity change (t-test with $p < 0.05$, FWE corrected). Visualized using BrainNet [27].

	Path Length (L)		**Clustering Coefficient (C)**	
Binary	Pre	Post	Pre	Post
Whole Brain	1.3147	1.3021	0.8223	0.8231
DMN	2.1670	2.0118	0.7092	0.6621
CEN	1.8636	1.9017	0.5770	0.5928
Weighted	Pre	Post	Pre	Post
Whole Brain	3.0238	3.2967	0.3323	0.2810
DMN	2.6761	2.9988	0.3385	0.2673
CEN	3.8524	3.9476	0.1593	0.1593

TABLE I
GRAPH PARAMETERS.

B. Graph parameters

The calculated graph parameters for the whole brain, the DMN and the CEN are shown in Table I.

The binary path length L of the DMN showed a decrease, the clustering coefficient C showed a small decrease. The L and the C of the CEN showed a small increase. The whole brain parameters did not indicate an effect. The weighted L showed for all three cases an increase. The two weighted C's for the whole brain and the DMN showed a small decrease. The C of the CEN was not affected.

C. Seed-to-voxel analysis in DMN and CEN

The difference in seed-to-voxel analysis between the DLPFC and the DMN is shown in Figure 7, the DLPFC to CEN is shown in Figure 8. The FC change between the DLPFC and the DMN showed a mixed effect. Some areas showed an increase in FC, others a decrease. On average the connectivity was increased. The FC change between the DLPFC and the CEN showed an increase close to the DLPFC but a decrease in the rest of the network. This indicated a decreased connectivity between the separate areas of the CEN. The average connectivity however showed an increase.

V. Discussion

A. Results

An analysis pipeline was generated and tested based on one dataset. The single subject study showed a decreased connectivity after TMS. The connectivity change per node

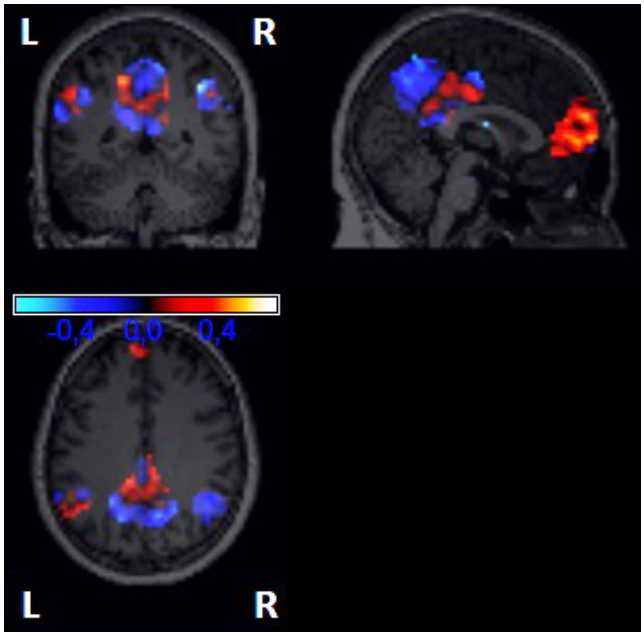

Fig. 7. The difference in correlation for masked seed-to-voxel analysis, shown in Fisher's z-transformed correlation coefficient as post TMS minus pre TMS. The difference in calculation between the TMS seed, the left dorsolateral prefrontal cortex, and all voxels in the Default Mode Network.

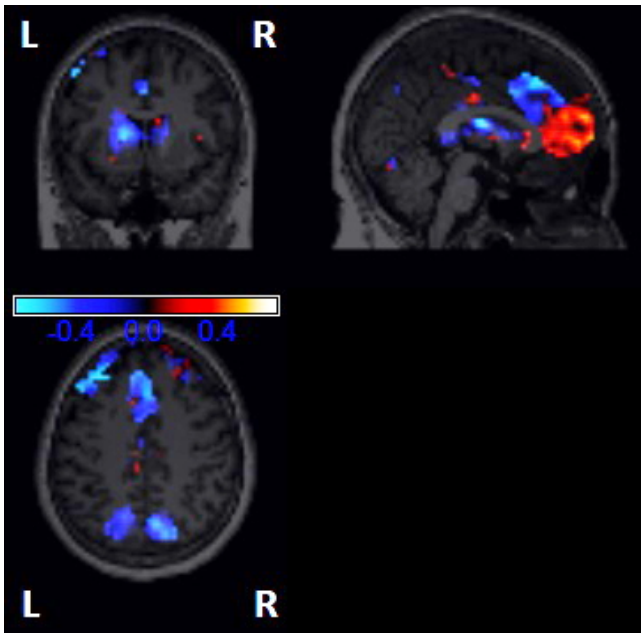

Fig. 8. The difference in correlation for masked seed-to-voxel analysis, shown in Fisher's z-transformed correlation coefficient as post TMS minus pre TMS. The difference in calculation between the TMS seed, the left dorsolateral prefrontal cortex, and all voxels in the Central Executive Network.

showed a change in connectivity which spread across the brain. This was in line with the whole brain weighted parameters where L showed an increase and the C a decrease, which could indicate a decreased connectivity. However, the study did not indicate an effect on the binary C and L for the entire brain. For the DMN the weighted parameters showed an increased L and decreased C. The binary L was decreased. The weighted L for the CEN showed a small increase. This might have indicated that the effect of TMS mainly affects the DMN network and that there is no effect present on the CEN. Also it indicated that weighted graph parameters might be a better measure for connectivity change then binary parameters. To verify this the analysis of more subjects is required.

Seed-to-voxel analysis indicated a decreased connectivity within the CEN except for the region close to the DLPFC after TMS and an average increased connectivity. A study by Liston et al. with a similar analyis showed no changes in the CEN [12]. This is more in line with our graph parameters of the CEN which showed a minor increase in L. The average connectivity between the DLPFC and the DMN was decreased in our study, but local increases and decreases were visible. Liston et al. found a less elevated connectivity after TMS [12]. This seems in contrast with the decrease in L for the binary graph. It is more in line with the weighted graph parameters: our DMN parameters showed less connectivity with increased L and decreased C. But the parameter differences are very small so further research of more subjects is needed.

It could be possible that the effect was no longer visible in the scan since the subject was not scanned immediately after the stimulation and the duration of the effect of TMS is not exactly known. However in a study by Pascual-Leone et al. it was shown that the effect on depressive symptoms tapered off over 14 days [14]. Therefore we expected the effect to still be visible.

B. Methodology

The FC over the whole brain was investigated by use of the Brodmann atlas. The correlation between neighboring voxels was high, but this decreased very fast when the distance between the voxels increased. The variance in time series within a BA was high and this could indicate that the Brodmann atlas did not properly represent the functional areas. Use of smaller regions might give a better insight in the FC. Areas derived from the data by using clusters of voxels that have similar time series for example. However, too small areas such as full brain voxel-to-voxel analysis would be difficult to interpret.

The seed signal, which was defined as the average of the time series in two BA's, is also affected by the variance in time series in the BA's. The two BA's of the seed formed an elongated area that stretches over a third of the outline of the left hemisphere. The seed signal could be improved by having a more accurate location of the stimulation position and using a smaller area to determine the average time series. Using neuronavigation the stimulation position could be determined within centimeter accuracy such that a smaller area for the seed area could be selected.

As a connectivity measure Pearson's correlation coefficient was used. There are other measures that might be used, such as partial correlation or coherence. Correlation and coherence methods perform better for fMRI than methods based on higher order statistics and partial correlation shows good results [20]. Partial correlation can be used as a method to separate the direct connections from the indirect connections by correcting for the effect of all other signals. For comparing

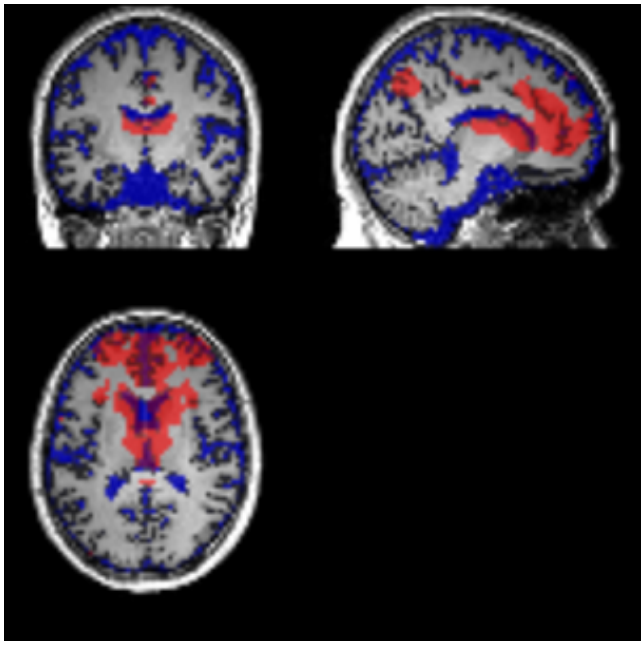

Fig. 9. The central executive network mask from Smith is shown in red, the CSF is shown in blue. The mask contains voxels in the CSF where no signal of interest is expected and therefore these voxels should not be used in the analysis.

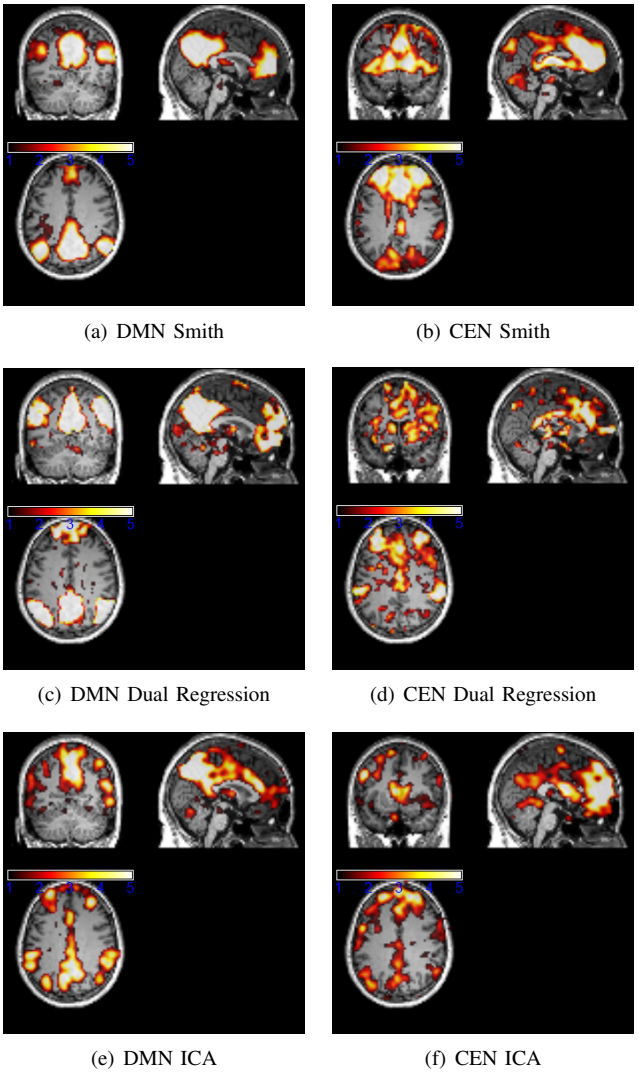

(a) DMN Smith (b) CEN Smith

(c) DMN Dual Regression (d) CEN Dual Regression

(e) DMN ICA (f) CEN ICA

Fig. 10. For both the Default Mode Network and the Central Executive Network three masks are shown. The first row shows the masks from Smith [19]. The second row shows the same networks after dual regression is applied. The last row shows the components determined using Independent Component Analysis that best match the reference networks. The shown slices are (34, 32, 44) and (34, 54, 44) for the DMN and CEN respectively. All masks are thresholded at Z=1.

the connectivity it is unnecessary to determine only direct connections. By using the WM and CSF signals as regressors, a large part of the background signal was already removed and there is less need for partial correlation, but the use of other measures could be investigated.

1) Masks: Another point of discussion are the used masks for the DMN and the CEN. When simply overlying the Smith masks on the normalized fMRI brain, these masks contain voxels in the CSF, as shown in Figure 9. In the CSF no cell bodies are present and the signals measured there are not directly caused by brain activity. Therefore the signals originating there are not of interest for this analysis and these voxels should not be present in the masks. To determine the effect of the CSF voxels, a mask was created from the Smith mask, without patient specific information, where the voxels that are present in the patient specific binary segmented CSF mask were left out. The patient specific segmented CSF image was transformed into a binary mask where all the voxels in the CSF image with a higher value then 80 percent of the maximum were excluded. When the graph parameters were calculated over the adjusted Smith masks from which the CSF voxels were excluded, this had a small effect on the parameters as it increases the differences between pre and post by 0.01 to 0.02.

The Smith masks are average masks and were not matched to individual differences in the anatomy. To adjust the maps for an individual subject, dual regression was applied to the masks [1]. The spatial masks were used to generate subject specific spatial maps and associated time series. This was done by solving equation (6) and (7). First all 10 3-dimensional masks of the resting state networks from Smith [19] were used as spatial regressors to extract from the 4-dimensional fMRI data of the subject the time series corresponding to these masks (6). Then these time series were used as temporal regressors, together with the realigment parameters and the average WM and CSF signals, to extract from the same 4D subject dataset the subject specific spatial maps (7). These maps could be thresholded and used as masks.

$$[\text{fMRI data}] = [\text{Smith masks}] \cdot [\text{time series}] \quad (6)$$

$$[\text{fMRI data}] = [\text{time series}] \cdot [\text{spatial maps}] \quad (7)$$

Another way to determine patient specific masks is by using independent component analysis (ICA) [2]. ICA was applied to the fMRI data using FSL's Melodic which decomposes the data into independent spatial and temporal components (8) [8]. The ICA maps were optimized to be statistically independent

and combined with the corresponding time series the original data is decomposed.

$$[\text{fMRI data}] = [\text{time series}] \cdot [\text{ICA maps}] \tag{8}$$

The data acquired pre TMS is used to extract 20 network components. The components with highest spatial correlation with the Smith DMN and CEN networks can be used as masks [19]. In Figure 10 the three determined masks for the DMN and the CEN are shown. The top row shows the masks from Smith [19]. The second row shows the masks after dual regression is applied. The last row shows the ICA components that had the highest spatial correlation with the Smith DMN and CEN masks.

After dual regression was applied the DMN mask looked similar to the Smith mask. However the activation region in the frontal area was moved to the outside where it overlaps with the CSF. This was also the case for the ICA component matching the DMN. The ICA component matching the CEN had some voxels in the skull. Using a higher threshold could solve this.

Another possibility is to use a mask derived from a seed region.This requires the localization of the seed, from which functionally connected regions are determined by using a generalized linear model. The determined functionally connected regions could be used as a mask.

Besides determining graph parameters in the masks derived from FC, it would be interesting to create a mask derived from structural connectivity using diffusion tensor imaging (DTI) analysis. If the effect of TMS spreads by the structural connections, it could effect the graph parameters in the structurally connected regions. To investigate this a mask could be created that contains the areas that are structurally connected to the seed and determine the graph parameters from that mask.

2) Graph theory: Comparing graphs and graph parameters is not straightforward [24]. For weighted graphs, the difference in average weight might influence the derived parameters. Also the negative connections are not taken into account in the weighted graphs. This information could possibly be used.

The whole brain graph parameters were calculated for a sparsity level of 0.3 and the network parameters for a sparsity of 0.8. The choice of this level could affect the result. To investigate this effect, the graph parameters over a range of sparsity levels that result in connected graphs are shown in Figure 11. It could be seen that the sparsity has a minimal effect on the difference between the pre and post parameters for the whole brain and the CEN. However for the DMN, a higher sparsity resulted in a larger spread in graph parameters.

VI. Conclusions and Recommendations

An analysis pipeline was created which preprocesses the fMRI data and calculates FC parameters.

The results of a single dataset indicate an effect of TMS on the FC. The data showed a decreased overall connectivity and the connectivity change per node indicated that the effect spreads across the brain. The binary graph parameters over the entire brain showed no effect. The DMN showed a slightly decreased L after TMS. The other parameter differences were

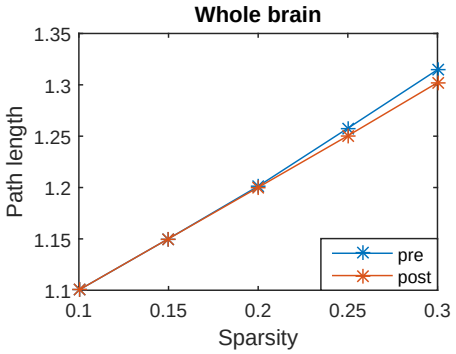

(a) Whole brain: L

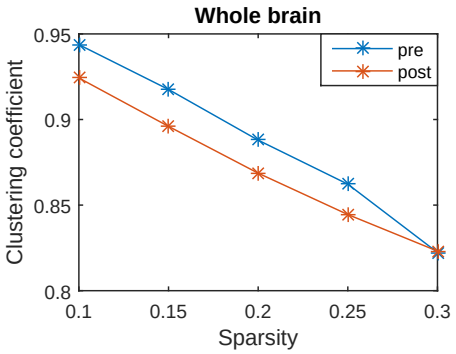

(b) Whole brain: C

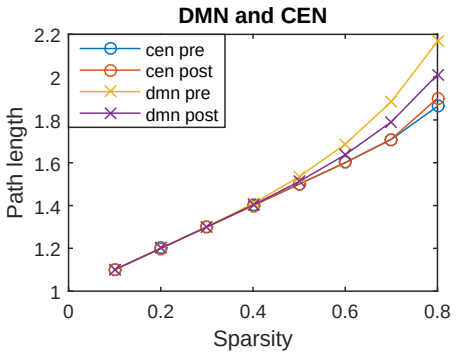

(c) DMN and CEN: L

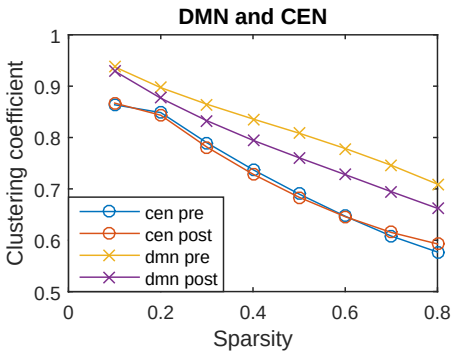

(d) DMN and CEN: C

Fig. 11. The effect of the sparsity on the graph parameters path length L and clustering coefficient C is shown. In (a) and (b) the whole brain parameters show no effect of sparsity. In (c) and (d), L and C calculated for the default mode network and the central executive network, the graphs show an increased sparsity results in an increased difference between the parameters.

small and the analysis of more subjects is needed before conclusions can be drawn.

The seed-to-voxel analysis showed a decreased connectivity between the frontal area and the rest of the CEN, which might indicate a decreased connectivity within the CEN.

Further research is needed and more subjects should be analyzed. Using a better defined seed region would improve the analysis. Also the effect of TMS on the structural connectivity could be investigated.

APPENDIX
MATRIX INDICES TO BRODMANN AREA'S

Index	BA	Index	BA
1	BA.1 (L)	43	BA.33 (L)
2	BA.1 (R)	44	BA.33 (R)
3	BA.10 (L)	45	BA.34 (L)
4	BA.10 (R)	46	BA.34 (R)
5	BA.11 (L)	47	BA.35 (L)
6	BA.11 (R)	48	BA.35 (R)
7	BA.13 (L)	49	BA.36 (L)
8	BA.13 (R)	50	BA.36 (R)
9	BA.17 (L)	51	BA.37 (L)
10	BA.17 (R)	52	BA.37 (R)
11	BA.18 (L)	53	BA.38 (L)
12	BA.18 (R)	54	BA.38 (R)
13	BA.19 (L)	55	BA.39 (L)
14	BA.19 (R)	56	BA.39 (R)
15	BA.2 (L)	57	BA.4 (L)
16	BA.2 (R)	58	BA.4 (R)
17	BA.20 (L)	59	BA.40 (L)
18	BA.20 (R)	60	BA.40 (R)
19	BA.21 (L)	61	BA.41 (L)
20	BA.21 (R)	62	BA.41 (R)
21	BA.22 (L)	63	BA.42 (L)
22	BA.22 (R)	64	BA.42 (R)
23	BA.23 (L)	65	BA.43 (L)
24	BA.23 (R)	66	BA.43 (R)
25	BA.24 (L)	67	BA.44 (L)
26	BA.24 (R)	68	BA.44 (R)
27	BA.25 (L)	69	BA.45 (L)
28	BA.25 (R)	70	BA.45 (R)
29	BA.27 (L)	71	Seed (L)
30	BA.27 (R)	72	BA.46 (R)
31	BA.28 (L)	73	BA.47 (L)
32	BA.28 (R)	74	BA.47 (R)
33	BA.29 (L)	75	BA.5 (L)
34	BA.29 (R)	76	BA.5 (R)
35	BA.3 (L)	77	BA.6 (L)
36	BA.3 (R)	78	BA.6 (R)
37	BA.30 (L)	79	BA.7 (L)
38	BA.30 (R)	80	BA.7 (R)
39	BA.31 (L)	81	BA.8 (L)
40	BA.31 (R)	82	BA.8 (R)
41	BA.32 (L)	83	BA.9 (R)
42	BA.32 (R)		

REFERENCES

[1] C. F. Beckmann, C. E. Mackay, N. Filippini, and S. M. Smith. Group comparison of resting-state FMRI data using multi-subject ICA and dual regression. *NeuroImage*, 47:S148, 2009.

[2] C. F. Beckmann and S. M. Smith. Probabilistic Independent Component Analysis for Functional Magnetic Resonance Imaging. *IEEE Transactions on Medical Imaging*, 23(2):137–152, 2004.

[3] Y. Behzadi, K. Restom, J. Liau, and T. T. Liu. A component based noise correction method (CompCor) for BOLD and perfusion based fMRI. *NeuroImage*, 37(1):90–101, 2007.

[4] K. Brodmann. *Brodmann's: Localisation in the Cerebral Cortex*. Springer New York, 2005.

[5] L. Douw, M. de Groot, E. van Dellen, J. J. Heimans, H. E. Ronner, C. J. Stam, and J. C. Reijneveld. 'Functional Connectivity' Is a Sensitive Predictor of Epilepsy Diagnosis after the First Seizure. *PLoS ONE*, 5(5):1–7, 2010.

[6] M. D. Greicius, B. H. Flores, V. Menon, G. H. Glover, H. B. Solvason, H. Kenna, A. L. Reiss, and A. F. Schatzberg. Resting-State Functional Connectivity in Major Depression: Abnormally Increased Contributions from Subgenual Cingulate Cortex and Thalamus. 62(5):429–437, 2007.

[7] Y. Z. Huang, M. J. Edwards, E. Rounis, K. P. Bhatia, and J. C. Rothwell. Theta burst stimulation of the human motor cortex. *Neuron*, 45(2):201–206, 2005.

[8] M. Jenkinson, C. F. Beckmann, T. E. J. Behrens, M. W. Woolrich, and S. M. Smith. Fsl. *NeuroImage*, 62(2):782–790, 2012.

[9] A. Khazaee, A. Ebrahimzadeh, and A. Babajani-Feremi. Identifying patients with Alzheimers disease using resting-state fMRI and graph theory. *Clinical Neurophysiology*, 2015.

[10] V. K. Kimiskidis. Transcranial Magnetic Stimulation for Drug-Resistant Epilepsies: Rationale and Clinical Experience. *European Neurology*, 63:205–210, 2010.

[11] Y. Kuroda, N. Motohashi, H. Ito, S. Ito, A. Takano, T. Nishikawa, and T. Suhara. Effects of repetitive transcranial magnetic stimulation on [11C]raclopride binding and cognitive function in patients with depression. *Journal of affective disorders*, 95(1-3):35–42, Oct. 2006.

[12] C. Liston, A. C. Chen, B. D. Zebley, A. T. Drysdale, R. Gordon, B. Leuchter, H. U. Voss, B. J. Casey, A. Etkin, and M. J. Dubin. Default Mode Network Mechanisms of Transcranial Magnetic Stimulation in Depression. *Biological Psychiatry*, 76(7):517–526, 2014.

[13] H. S. Mayberg, A. M. Lozano, V. Voon, H. E. McNeely, D. Seminowicz, C. Hamani, J. M. Schwalb, and S. H. Kennedy. Deep brain stimulation for treatment-resistant depression. *Neuron*, 45(5):651–660, 2005.

[14] A. Pascual-Leone, B. Rubio, F. Pallardó, and M. D. Catalá. Rapid-rate transcranial magnetic stimulation of left dorsolateral prefrontal cortex in drug-resistant depression. *Lancet*, 348(9022):233–237, 1996.

[15] P. M. Rossini, L. Rossini, and F. Ferreri. Brain-behavior relations: transcranial magnetic stimulation: a review. *IEEE engineering in medicine and biology magazine : the quarterly magazine of the Engineering in Medicine & Biology Society*, 29(1):84–95, 2010.

[16] M. Rubinov and O. Sporns. Complex network measures of brain connectivity: Uses and interpretations. *NeuroImage*, 52(3):1059–69, Sept. 2010.

[17] T. V. Salomons, K. Dunlop, S. H. Kennedy, A. Flint, J. Geraci, P. Giacobbe, and J. Downar. Resting-State Cortico-Thalamic-Striatal Connectivity Predicts Response to Dorsomedial Prefrontal rTMS in Major Depressive Disorder. *Neuropsychopharmacology*, 39(2):488–498, 2013.

[18] M. M. Shafi, M. Brandon Westover, L. Oberman, S. S. Cash, and A. Pascual-Leone. Modulation of EEG functional connectivity networks in subjects undergoing repetitive transcranial magnetic stimulation. *Brain topography*, 27(1):172–91, Jan. 2014.

[19] S. M. Smith, P. T. Fox, K. L. Miller, D. C. Glahn, P. M. Fox, C. E. Mackay, N. Filippini, K. E. Watkins, R. Toro, A. R. Laird, and C. F. Beckmann. Correspondence of the brain's functional architecture during activation and rest. *Proceedings of the National Academy of Sciences of the United States of America*, 106:13040–13045, 2009.

[20] S. M. Smith, K. L. Miller, G. Salimi-Khorshidi, M. Webster, C. F. Beckmann, T. E. Nichols, J. D. Ramsey, and M. W. Woolrich. Network modelling methods for FMRI. *NeuroImage*, 54(2):875–91, Jan. 2011.

[21] C. J. Stam, B. F. Jones, G. Nolte, M. Breakspear, and P. Scheltens. Small-world networks and functional connectivity in Alzheimer's disease. *Cerebral Cortex*, 17(1):92–99, Jan. 2007.

[22] G. Thut and A. Pascual-Leone. A review of combined TMS-EEG studies to characterize lasting effects of repetitive TMS and assess their usefulness in cognitive and clinical neuroscience. *Brain Topography*, 22(4):219–232, Jan. 2010.

[23] a. S.-c. R. Trial, M. S. George, S. H. Lisanby, D. Avery, W. M. Mcdonald, and V. Durkalski. Daily Left Prefrontal Transcranial Magnetic Stimulation Therapy for Major Depressive Disorder. 67(5):507–516, 2010.

[24] B. C. M. van Wijk, C. J. Stam, and A. Daffertshofer. Comparing brain networks of different size and connectivity density using graph theory. *PLoS ONE*, 5(10), 2010.

[25] D. J. Watts and S. H. Strogatz. Collective dynamics of small-world networks. *Nature*, 393(June):440–442, 1998.
[26] S. Whitfield-Gabrieli and A. Nieto-Castanon. Conn: a functional connectivity toolbox for correlated and anticorrelated brain networks. *Brain connectivity*, 2(3):125–41, Jan. 2012.
[27] M. Xia, J. Wang, and Y. He. BrainNet Viewer: a network visualization tool for human brain connectomics. *PloS one*, 8(7):e68910, Jan. 2013.
[28] L. L. Zeng, H. Shen, L. Liu, L. Wang, B. Li, P. Fang, Z. Zhou, Y. Li, and D. Hu. Identifying major depression using whole-brain functional connectivity: A multivariate pattern analysis. *Brain*, 135(5):1498–1507, 2012.